

# Dual-Peptide-Functionalized Albumin-Based Nanoparticles with pH-Dependent Self-Assembly Behavior for Drug Delivery

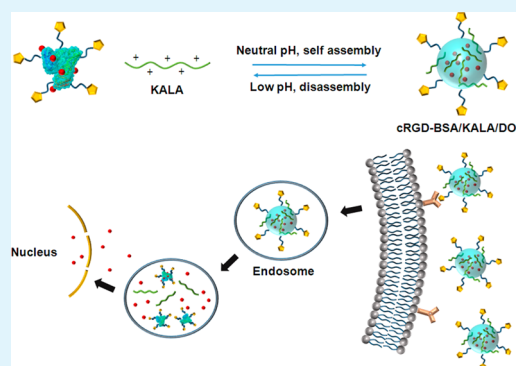
Bin Chen, Xiao-Yan He, Xiao-Qing Yi, Ren-Xi Zhuo, and Si-Xue Cheng\*

Key Laboratory of Biomedical Polymers of Ministry of Education, Department of Chemistry, Wuhan University, Wuhan, Hubei, People's Republic of China

## S Supporting Information

**ABSTRACT:** Drug delivery has become an important strategy for improving the chemotherapy efficiency. Here we developed a multi-functionalized nanosized albumin-based drug-delivery system with tumor-targeting, cell-penetrating, and endolysosomal pH-responsive properties. cRGD-BSA/KALA/DOX nanoparticles were fabricated by self-assembly through electrostatic interaction between cell-penetrating peptide KALA and cRGD-BSA, with cRGD as a tumor-targeting ligand. Under endosomal/lysosomal acidic conditions, the changes in the electric charges of cRGD-BSA and KALA led to the disassembly of the nanoparticles to accelerate intracellular drug release. cRGD-BSA/KALA/DOX nanoparticles showed an enhanced inhibitory effect in the growth of  $\alpha_v\beta_3$ -integrin-overexpressed tumor cells, indicating promising application in cancer treatments.

**KEYWORDS:** albumin, cell-penetrating peptide, self-assembly, nanoparticles, drug delivery, blood–brain barrier



Drug-delivery systems (DDSs), which have competitive advantages compared with conventional formulations, are of special importance in cancer treatments. Nanosized DDSs can be accumulated in tumor sites through the enhanced permeability and retention effect.<sup>1,2</sup> More importantly, through the introduction of targeting ligands, drug carriers can be preferably delivered to tumor sites to optimize the therapeutic efficiency.<sup>3–6</sup>

In this study, we developed a dual-peptide-functionalized albumin-based DDS, cRGD-BSA/KALA/DOX nanoparticles loaded with an antitumor drug (doxorubicin hydrochloride, DOX), for tumor-targeting delivery and evaluated its delivery efficiency using U87-MG glioblastoma cells. As we know, the blood–brain barrier (BBB) is a barrier formed between plasma brain capillaries and glial cells, preventing the entrance of some harmful substances into brain cells. However, in drug delivery, BBB results in poor penetration for chemotherapeutics from vessels into brain tumors, leading to the failure of chemotherapy. As the most common and aggressive brain tumor in humans, glioblastoma multiforme (GBM) is still one of the greatest challenges in cancer therapy because of the difficulty in drug delivery caused by BBB. To solve this problem, we incorporated a cyclic Arg-Gly-Asp (cRGD) peptide with selective affinity for  $\alpha_v\beta_3$  and  $\alpha_v\beta_5$  integrins overexpressed on the endothelial cells of tumor angiogenic vessels and GBM cells to the drug carrier.<sup>7</sup>

Among numerous drug carriers, albumin is an ideal carrier for diverse drug delivery because it has unique advantages including favorable biocompatibility, biodegradability, absorbability, nonantigenicity, nonimmunogenicity, preferential up-

take in tumor tissues, and good in vivo stability.<sup>8,9</sup> In addition, various drugs can be loaded into the albumin-based carriers because of the existence of different drug binding sites in albumin molecules.<sup>10–12</sup>

In this study, we demonstrated a novel albumin-based DDS possessing tumor-targeting, cell-penetrating, and endolysosomal pH-responsive properties (Scheme 1A) for cancer treatments. To achieve tumor-targeting drug delivery, cRGD was conjugated to bovine serum albumin (BSA) to form cRGD-BSA. Then an antineoplastic drug, DOX, was loaded into cRGD-BSA via hydrophilic and hydrophobic contacts to form stable cRGD-BSA/DOX complexes, which were further stabilized by hydrogen bonding.<sup>13</sup> After that, positively charged cell-penetrating peptide (CCP) KALA and negatively charged cRGD-BSA/DOX self-assembled into dual-functionalized albumin-based nanoparticles (cRGD-BSA/KALA/DOX) via electrostatic interactions.

After cell internalization mediated by a cRGD peptide, cRGD-BSA/KALA/DOX nanoparticles entered the acidic endolysosomes. Because the pH value decreased and approached the isoelectric point of BSA (pI = 4.7), the negative surface charge density of albumin decreased significantly. The decreased electrostatic interaction between BSA and KALA led to the disassembly of nanoparticles (Scheme 1B). In other words, the pH-dependent self-assembly and disassembly of our

Received: May 5, 2015

Accepted: July 10, 2015

Published: July 13, 2015

Scheme 1. (A) Structure and Formation of cRGD-BSA/KALA/DOX Nanoparticles and (B) Schematic Illustration of the Efficient Delivery of DOX to Nuclei for Cancer Therapy: Cell Uptake Mediated by cRGD, Internalization in Endosomes, Endolysosomal pH-Triggered Disassembly To Accelerate DOX Release, and Accumulation of DOX in the Cell Nucleus

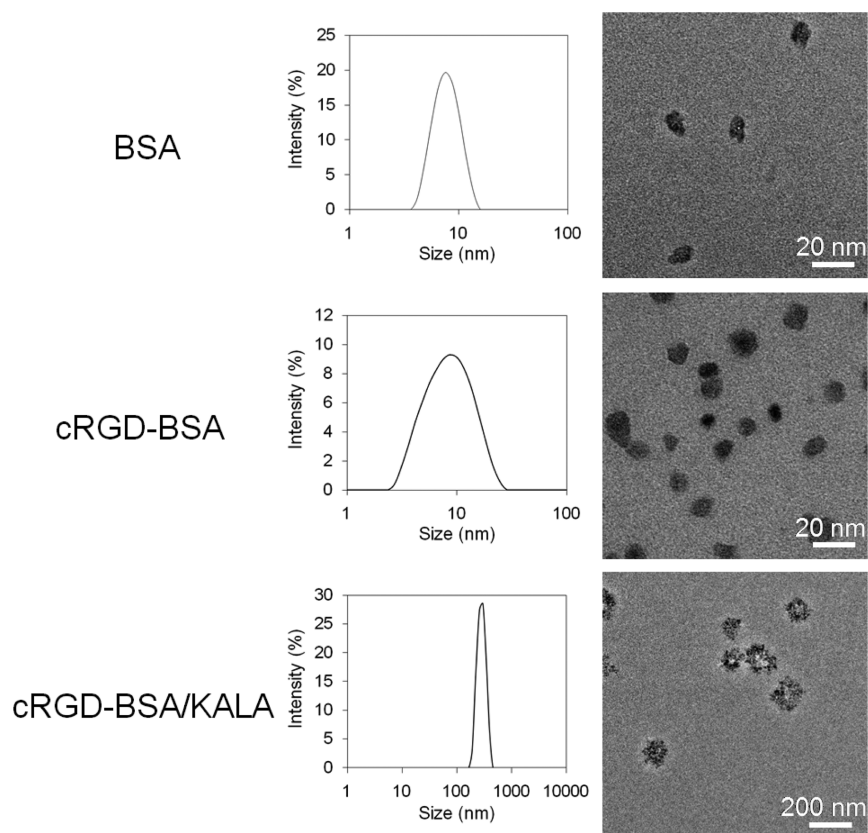
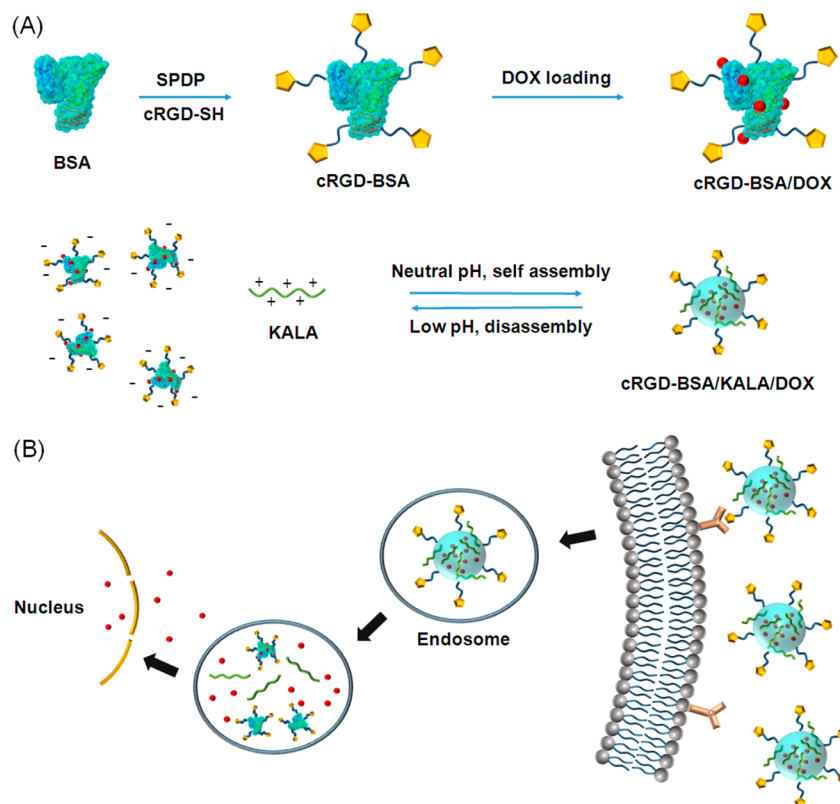
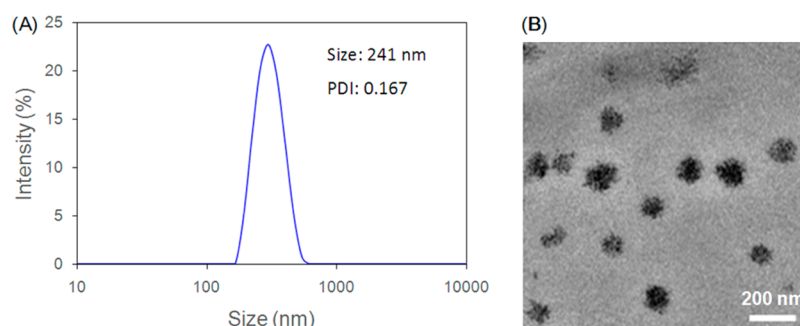
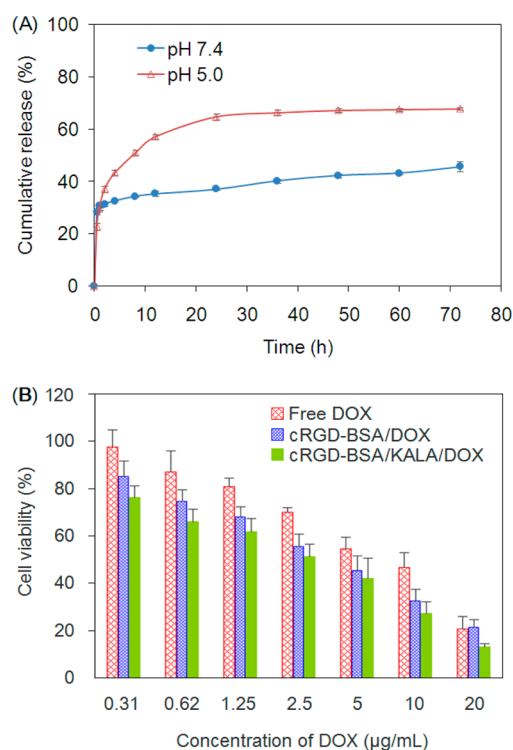


Figure 1. Size distributions and TEM images of BSA, cRGD-BSA, and blank cRGD-BSA/KALA nanoparticles.



**Figure 2.** (A) Size distribution and (B) TEM image of cRGD-BSA/KALA/DOX nanoparticles.



**Figure 3.** (A) In vitro DOX release from cRGD-BSA/KALA/DOX nanoparticles at pH 7.4 and 5.0. (B) Cell viability of U87-MG cells after treatment with free DOX, cRGD-BSA/DOX, and cRGD-BSA/KALA/DOX for 48 h.

delivery vehicle could be activated by the cellular environment to achieve accelerated intracellular drug release.

In our study, a cRGD peptide was incorporated into BSA to endow the delivery vehicle with a tumor-targeting property. To synthesize cRGD-BSA, the amino groups of BSA were reacted with the bifunctional cross-linker *N*-succinimidyl 3-(2-pyridyldithio)propionate (SPDP). Then cRGD-SH reacted with the SPDP-conjugated albumin to form cRGD-BSA through a thiol exchange reaction (Figure S1 in the Supporting Information, SI).

Approximately 4–5 cRGD molecules were linked to each BSA molecule, which was determined by UV spectroscopy based on the release of the colored product pyridine-2-thione (Figure S1 in the SI).

Far-UV circular dichroism (CD) was employed to characterize the secondary structures of native BSA and cRGD-BSA. For BSA before cRGD modification,  $\alpha$ -helix and  $\beta$ -sheet structures were observed (Figure S2A in the SI). Generally, the  $\alpha$ -helix had negative ellipticity at 222 and 208 nm, whereas the  $\beta$ -sheet

showed a negative band at 218 nm. After reaction, structural perturbations on both the  $\alpha$ -helix and  $\beta$ -sheet could be detected for cRGD-BSA, indicating that cRGD was linked to BSA successfully. In addition, matrix-assisted laser desorption/ionization time-of-flight mass spectrometry characterization also confirmed the conjugation of cRGD to BSA (Figure S2B in the SI). Dynamic laser light scattering (DLS) and transmission electron microscopy (TEM) indicated that cRGD modification did not result in apparent changes in the size, zeta potential, and morphology compared with native BSA because of the relatively small size of cRGD (Table S1 in the SI and Figure 1). No obvious difference in the sizes of BSA and cRGD-BSA could be detected by DLS and TEM because BSA had a defined three-dimensional structure.

CPPs have been extensively explored for enhancing the cell uptake and nuclear translocation of biopharmaceuticals such as peptides, proteins, or nucleic acids.<sup>14–16</sup> Among the numerous CPPs, KALA is a cationic CCP that is able to destabilize lipid membranes and facilitate cellular entry. In addition, the membrane-disruptive KALA undergoes a conformational change in a pH-dependent manner, which results in enhanced endolysosomal escape due to the low-pH environment in endolysosomes.<sup>17</sup> The presence of KALA in DDSs could effectively improve the delivery efficiency.<sup>18</sup> More importantly, the molecular weight of KALA is high enough for self-assembly and can form stable complexes with negatively charged cRGD-BSA through electrostatic interactions. So in this study, KALA was identified and used to enhance the delivery efficiency of the DDS. According to previous studies, CPPs can effectively deliver BSA into cells through noncovalent association as a form of BSA/ CPP complexes.<sup>19</sup> Inspired by the ideas above, we prepared cRGD-BSA/KALA complexes by self-assembly via electrostatic interactions between positively charged KALA and negatively charged cRGD-BSA.

To optimize the stoichiometry for complex formation, different amounts of KALA peptide were mixed with cRGD-BSA in the absence of DOX (cRGD-BSA/KALA molar ratios of 1:1, 2:1, 4:1, and 8:1). The size of the particles was monitored by DLS for 48 h (Figure S3 in the SI). It was found that a low cRGD-BSA/KALA ratio (1:1 or 2:1) resulted in the formation of large irregular aggregates, and precipitation occurred after 2 days. In contrast, a high cRGD-BSA/KALA ratio (8:1) could not form enough nanoparticles after centrifugation. Because a cRGD-BSA/KALA ratio at 4:1 resulted in stable nanosized complexes, the ratio was fixed at 4:1 for further study. The TEM image showed that cRGD-BSA/KALA nanoparticles had a spherical shape with a size of less than 200 nm (Figure 1). Compared with the dried cRGD-BSA/KALA nanoparticles observed by TEM, the size of the

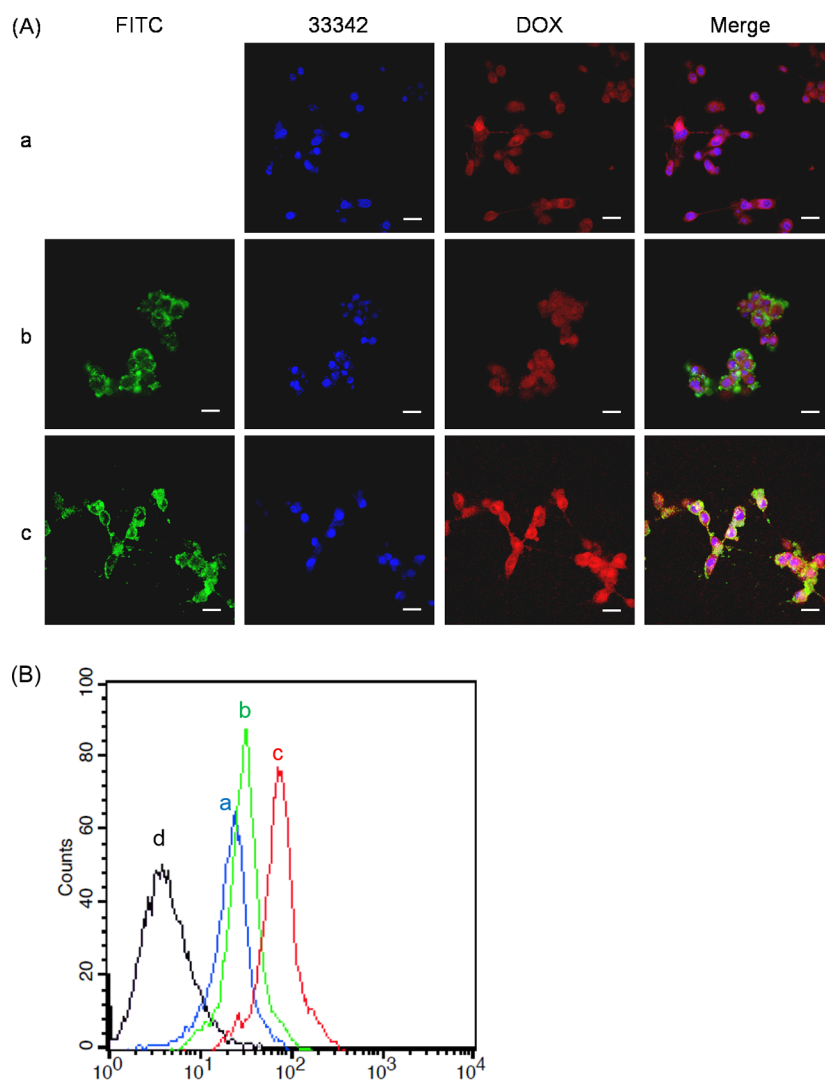


**Figure 4.** (A) CLSM images and (B) flow cytometry analysis of U87-MG cells after different treatments: (a) free DOX; (b) cRGD-BSA/DOX; (c) cRGD-BSA/KALA/DOX; (d) control without any treatment. Scale bar: 20  $\mu\text{m}$ . The concentration of DOX was fixed at 10  $\mu\text{g/mL}$ , and the coincubation time was 4 h. cRGD-BSA was labeled by FITC. Cell nuclei were stained with Hoechst 33342.

nanoparticles in aqueous media measured by DLS was larger because the complexed nanoparticles were hydrolyzed and swollen in water. As we know, albumin-based delivery systems have good physiological stability because albumin is a plasma protein. In our study, we also found that our albumin-based delivery systems were stable in the media with the presence of ions and serum.

The pH sensitivity is a favorable function for DDS, which may result in the effective drug release in acid cell organelles such as endosomes and lysosomes. Interestingly, our cRGD-BSA/KALA nanoparticles exhibited pH-dependent self-assembly behavior; i.e., cRGD-BSA/KALA complexes formed at neutral pH and disassembled at acidic pH. To study the disassembly of cRGD-BSA/KALA nanoparticles under acidic conditions, cRGD-BSA/KALA nanoparticles prepared at neutral pH were transferred and suspended in acetic acid buffer (pH 5.0) to monitor the size and size distribution changes. Under acidic conditions, the particle size gradually decreased, and cRGD-BSA/KALA complexes finally changed to individual cRGD-BSA and KALA molecules, indicating the occurrence of disassembly (Figure S4 in the SI).

To confirm the tumor-targeting property of cRGD and enhanced cell uptake of KALA, the cells after different treatments were observed using confocal laser scanning microscopy (CLSM; Figure S5 in the SI). The confocal images indicated that cRGD-BSA could significantly enhance cell uptake compared with native BSA in U87-MG cells, while for NIH 3T3 cells with a low integrin expression, coincubation with cRGD-BSA did not result in obvious increased cell internalization. In addition, the intracellular accumulation of cRGD-BSA in U87-MG cells could be dramatically inhibited by excess free cRGD, which further suggested that enhanced cell uptake resulted from the specific interaction between cRGD and integrin overexpressed on the glioblastoma cells. In addition, the internalization of cRGD-BSA could be significantly inhibited at 4  $^{\circ}\text{C}$ , indicating that adenosine-triphosphate (ATP) was involved in the uptake process.<sup>20,21</sup> With the presence of KALA, significant enhanced green fluorescence (FITC-labeled cRGD-BSA) was observed in the cells treated by cRGD-BSA/KALA nanoparticles, confirming the increased cellular accumulation of internalized cRGD-BSA/KALA nanoparticles.

The size and morphology of drug-loaded cRGD-BSA/KALA/DOX nanoparticles (Figure 2) were close to those of blank cRGD-BSA/KALA nanoparticles (Figure 1). The encapsulation efficiency and drug loading content of DOX were determined to be 73.9% and 3.7%, respectively.

In vitro drug release from cRGD-BSA/KALA/DOX nanoparticles indicated that drug release was obviously accelerated at pH 5.0 compared with that at pH 7.4, which was mainly due to the weaker interaction between positively charged DOX molecules and negatively charged cRGD-BSA because more groups in cRGD-BSA were protonated at a decreased pH (Figure 3A).<sup>13</sup> In addition, the disassembly of nanoparticles at low pH also contributed to the fast release at pH 5.0.

We further estimated the cytotoxicity of the different agents against U87-MG cells (Figure 3B). Dose-dependent antitumor activities could be observed for both free DOX and drug-loaded nanoparticles. In vitro assays demonstrated that cRGD and KALA dual peptide modification led to significant improvement in the anticancer efficiency in U87-MG cells. Compared with free DOX, cRGD-BSA/DOX nanoparticles resulted in a stronger tumor cell inhibition, which was mainly due to enhanced cell uptake mediated by cRGD moieties on the nanoparticle surface. With the versatile functions (cell penetrating and endolysosomal escaping) of KALA peptide, dual-functionalized cRGD-BSA/KALA/DOX nanoparticles exhibited significantly higher cytotoxicity ( $IC_{50} = 2.6 \mu\text{g/mL}$ ) compared with free DOX ( $IC_{50} = 9.4 \mu\text{g/mL}$ ). However, it should be noted that the overall difference between cRGD-BSA/KALA/DOX and cRGD-BSA/DOX nanoparticles ( $IC_{50} = 4.1 \mu\text{g/mL}$ ) was not dramatic. Because the cell viability was evaluated after coincubation with drug-loaded nanoparticles for 48 h, the time interval was enough for cell internalization and drug release to inhibit the cell growth.

The cellular internalization and intracellular localization of different agents in U87-MG cells were studied using CLSM after treatment for 4 h (Figure 4A). Notably, compared with the treatments by free DOX and cRGD-BSA/DOX, the CLSM images showed a significantly higher intracellular DOX accumulation (red fluorescence) for the cells treated by cRGD-BSA/KALA/DOX nanoparticles. The colocalization of red and green fluorescences demonstrated that the increased intracellular DOX concentration was caused by the efficient delivery of cRGD-BSA/KALA/DOX nanoparticles. Because of the enhanced endolysosomal escape with the help of KALA, DOX was quickly released into the cytoplasm and subsequently localized in nuclei. Flow cytometric analysis, which detected the intracellular red fluorescence from DOX, further confirmed that the DOX concentration in U87-MG cells treated by cRGD-BSA/KALA/DOX nanoparticles was highest (Figure 4B). The results of CLSM and flow cytometry were in accordance with the cell inhibitory effect determined by MTT assay.

In summary, an albumin-based DDS possessing tumor-targeting, cell-penetrating, and endolysosomal pH-responsive properties was successfully prepared via the self-assembly between cRGD-BSA and KALA peptide. The cRGD-BSA/KALA/DOX nanoparticles showed significantly enhanced cell internalization due to the integrin targeting of cRGD and the cell-penetrating effect of KALA. More importantly, the nanoparticles could respond to endosomal or lysosomal acidity because of the pH-triggered disassembly of cRGD-BSA/KALA complexes to release DOX quickly and to efficiently inhibit tumor cell growth. This smart DDS represents an important

strategy for efficiently promoting therapeutic efficacy in cancer treatments.

## ■ ASSOCIATED CONTENT

### Supporting Information

Experimental details and additional figures. The Supporting Information is available free of charge on the ACS Publications website at DOI: 10.1021/acsami.5b03866.

## ■ AUTHOR INFORMATION

### Corresponding Author

\*E-mail: chengsixue@whu.edu.cn. Fax: 86 (27) 68754509.

### Notes

The authors declare no competing financial interest.

## ■ ACKNOWLEDGMENTS

Financial support from the National Natural Science Foundation of China (Grant 21274113) is gratefully acknowledged.

## ■ REFERENCES

- (1) Li, C.; Li, K.; Yan, H. H.; Li, G. H.; Xia, J. S.; Wei, X. B. Dextran Based pH-Activated Near-infrared Fluorescence Nanoprobe Imaging the Acidic Compartments in Cancer Cells. *Chem. Commun.* **2010**, *46*, 1326–1328.
- (2) Guerrero-Cázares, H.; Tzeng, S. Y.; Young, N. P.; Abutaleb, A. O.; Quiñones-Hinojosa, A.; Green, J. J. Biodegradable Polymeric Nanoparticles Show High Efficacy and Specificity at DNA Delivery to Human Glioblastoma *in Vitro* and *in Vivo*. *ACS Nano* **2014**, *8*, 5141–5153.
- (3) Seo, J. H.; Kakinoki, S.; Inoue, Y.; Yamaoka, T.; Ishihara, K.; Yui, N. Inducing Rapid Cellular Response on RGD-Binding Threaded Macromolecular Surfaces. *J. Am. Chem. Soc.* **2013**, *135*, 5513–5516.
- (4) Ji, S. D.; Czerwinski, A.; Zhou, Y.; Shao, G. Q.; Valenzuela, F.; Sowiński, P.; Chauhan, S.; Pennington, M.; Liu, S. <sup>99m</sup>Tc-Galactose-RGD<sub>2</sub>: A Novel <sup>99m</sup>Tc-Labeled Cyclic RGD Peptide Dimer Useful for Tumor Imaging. *Mol. Pharmaceutics* **2013**, *10*, 3304–3314.
- (5) Kunjachan, S.; Pola, R.; Gremse, F.; Theek, B.; Ehling, J.; Moeckel, D.; Hermanns-Sachweh, B.; Pechar, M.; Ulbrich, K.; Hennink, W. E.; Storm, G.; Lederle, W.; Kiessling, F.; Lammers, T. Passive Versus Active Tumor Targeting Using RGD- and NGR-Modified Polymeric Nanomedicines. *Nano Lett.* **2014**, *14*, 972–981.
- (6) Zhen, Z. P.; Tang, W.; Chen, H. M.; Lin, X.; Todd, T.; Wang, G.; Cowger, T.; Chen, X. Y.; Xie, J. RGD-Modified Apoferritin Nanoparticles for Efficient Drug Delivery to Tumors. *ACS Nano* **2013**, *7*, 4830–4837.
- (7) Miura, Y.; Takenaka, T.; Toh, K.; Wu, S. R.; Nishihara, H.; Kano, M. R.; Ino, Y.; Nomoto, T.; Matsumoto, Y.; Koyama, H.; Cabral, H.; Nishiyama, N.; Kataoka, K. Cyclic RGD-Linked Polymeric Micelles for Targeted Delivery of Platinum Anticancer Drugs to Glioblastoma through the Blood-Brain Tumor Barrier. *ACS Nano* **2013**, *7*, 8583–8592.
- (8) Du, C. L.; Deng, D. W.; Shan, L. L.; Wan, S. N.; Cao, J.; Tian, J. M.; Achilefu, S.; Gu, Y. Q. A pH-Sensitive Doxorubicin Prodrug Based on Folate-Conjugated BSA for Tumor-Targeted Drug Delivery. *Biomaterials* **2013**, *34*, 3087–3097.
- (9) Ming, X.; Carver, K.; Wu, L. Albumin-Based Nanoconjugates for Targeted Delivery of Therapeutic Oligonucleotides. *Biomaterials* **2013**, *34*, 7939–7949.
- (10) Xie, J. B.; Cao, Y.; Xia, M.; Gao, X.; Qin, M.; Wei, J. W.; Wang, W. One-Step Photo Synthesis of Protein–Drug Nanoassemblies for Drug Delivery. *Adv. Healthcare Mater.* **2013**, *2*, 795–799.
- (11) Xu, R. Z.; Fisher, M.; Juliano, R. L. Targeted Albumin-Based Nanoparticles for Delivery of Amphipathic Drugs. *Bioconjugate Chem.* **2011**, *22*, 870–878.

- (12) Piradashvili, K.; Fichter, M.; Mohr, K.; Gehring, S.; Wurm, F. R.; Landfester, K. Biodegradable Protein Nanocontainers. *Biomacromolecules* **2015**, *16*, 815–821.
- (13) Chen, B.; Wu, C.; Zhuo, R. X.; Cheng, S. X. A Self-Assembled Albumin Based Multiple Drug Delivery Nanosystem to Overcome Multidrug Resistance. *RSC Adv.* **2015**, *5*, 6807–6814.
- (14) Sayers, E. J.; Cleal, K.; Eissa, N. G.; Watson, P.; Jones, A. T. Distal Phenylalanine Modification for Enhancing Cellular Delivery of Fluorophores, Proteins and Quantum Dots by Cell Penetrating Peptides. *J. Controlled Release* **2014**, *195*, 55–62.
- (15) Youngblood, D. S.; Hatlevig, S. A.; Hassinger, J. N.; Iversen, P. L.; Moulton, H. M. Stability of Cell-Penetrating Peptide-Morpholino Oligomer Conjugates in Human Serum and in Cells. *Bioconjugate Chem.* **2007**, *18*, 50–60.
- (16) Copolovici, D. M.; Langel, K.; Eriste, E.; Langel, Ü. Cell-Penetrating Peptides: Design, Synthesis, and Applications. *ACS Nano* **2014**, *8*, 1972–1994.
- (17) Wyman, T. B.; Nicol, F.; Zelphati, O.; Scaria, P. V.; Plank, C.; Szoka, F. C. Design, Synthesis, and Characterization of a Cationic Peptide That Binds to Nucleic Acids and Permeabilizes Bilayers. *Biochemistry* **1997**, *36*, 3008–3017.
- (18) Liang, P.; Liu, C. J.; Zhuo, R. X.; Cheng, S. X. Self-Assembled Inorganic/Organic Hybrid Nanoparticles with Multi-Functionalized Surfaces for Active Targeting Drug Delivery. *J. Mater. Chem. B* **2013**, *1*, 4243–4250.
- (19) Carter, E.; Lau, C. Y.; Tosh, D.; Ward, S. G.; Mrsny, R. J. Cell Penetrating Peptides Fail to Induce an Innate Immune Response in Epithelial Cells *in Vitro*: Implications for Continued Therapeutic Use. *Eur. J. Pharm. Biopharm.* **2013**, *85*, 12–19.
- (20) Li, Y.; Lin, J. Y.; Wu, H. J.; Chang, Y.; Yuan, C. H.; Liu, C.; Wang, S.; Hou, Z. Q.; Dai, L. Z. Orthogonally Functionalized Nanoscale Micelles for Active Targeted Codelivery of Methotrexate and Mitomycin C with Synergistic Anticancer Effect. *Mol. Pharmaceutics* **2015**, *12*, 769–782.
- (21) Lee, Y.; Graeser, R.; Kratz, F.; Geckeler, K. E. Paclitaxel-Loaded Polymer Nanoparticles for the Reversal of Multidrug Resistance in Breast Cancer Cells. *Adv. Funct. Mater.* **2011**, *21*, 4211–4218.